Breach and recurrence of dissipative soliton resonance during period doubling evolution in a fiber laser

Yufei Wang,[1,2] Lei Su,[2] Shuai Wang,[3] Limin Hua,[3] Lei Li,[3] Deyuan Shen,[3] Dingyuan Tang,[4] Andrey Komarov,[5] Mariusz Klimczak,[6,7] Songnian Fu,[1] Ming Tang,[1] Xiahui Tang,[1] and Luming Zhao[1,2,3,*]

[1] *School of Optical and Electronic Information and Wuhan National Laboratory for Optoelectronics, Huazhong University of Science and Technology, Wuhan 430074, People's Republic of China*

[2] *School of Engineering and Materials Science, Queen Mary University of London, London E1 4NS, UK*

[3] *Jiangsu Key Laboratory of Advanced Laser Materials and Devices, School of Physics and Electronic Engineering, Jiangsu Normal University, Xuzhou 221116, People's Republic of China*

[4] *School of Electrical and Electronic Engineering, Nanyang Technological University, Singapore 639798*

[5] *Institute of Automation and Electrometry, Russian Academy of Sciences, Novosibirsk 630090, Russia*

[6] *Faculty of Physics, University of Warsaw, Warsaw 02-093, Poland*

[7] *Institute of Electronic Materials Technology, Warsaw 01-919, Poland*

(Dated: May 18, 2020)

We reported the first experimental demonstration of period doubling of dissipative soliton resonance (DSR) pulses in a fiber laser. DSR occurs in the close vicinity consisting of a set of parameters of a dissipative system, where the energy of the generated soliton increases without limit while the pulse peak power is clamped. Consequently, DSR pulses are immune to appearance of period doubling, which is a threshold effect. However, period doubling of DSR pulses are experimentally demonstrated and numerically duplicated. The typical DSR feature, clamped pulse peak power and linear variation in pulse width with respect to the pump power change, is lost during the transition from period one to period doubling. However, the DSR performance reappears once the period doubling was fully developed. The breach and recurrence of DSR operation during pulse evolution is resulted from the simultaneous change of multiple parameters because of the increasing pump power. In addition, DSR pulse narrowing with pump power increasing under period-doubling state was experimentally observed.

I. INTRODUCTION

Passively mode-locked fiber lasers have been widely used in various applications because of their easily manageable structure and unparalleled performance. The study of pulse dynamics in fiber lasers is always a hot topic in recent decades. On the way of pursuing larger pulse energy, dissipative soliton resonance (DSR), a novel existence of pulse formation was discovered by Chang. et al in 2008 [1]. Based on numerical simulations of the cubic-quintic complex Ginzburg-Landau equation (CGLE), they found that there existed a parameter regime where the mode-locked pulse could maintain its peak power and linearly broaden its pulse width with the increase in the gain. Owing to the clamped pulse peak power, the pulse energy of the DSR pulse could be boosted arbitrarily without pulse breaking, which is much different from general solitons resulted from fiber lasers [2–4]. In 2009, Wu. et al first experimentally demonstrated the DSR pulse generation in a fiber laser by utilizing the nonlinear polarization rotation technique in the normal dispersion regime [5]. Following that, researchers further investigated the DSR pulse as a universal phenomenon that could be obtained under different cavity structures such as the figure-of-eight [6], figure-of-nine [7] and linear cavity [8], with various kinds of mode-locking techniques such as using the nonlinear optical loop mirror (NOLM) [9], using the nonlinear amplifying loop mirror [10] and using novel materials [11–13]. Recently, Song et al summarized research on DSR fiber lasers under the term of "Flat-top dissipative soliton" [4]. DSR-based fiber lasers have shown their great potential as a reliable source to generate pulses with ultra-high pulse energy. Semaan et al reported a single DSR pulse with 10 µJ pulse energy directly from a figure-of-eight double-clad Er:Yb co-doped fiber laser [14]. DSR lasers are also promising to serve as a seed source for fiber amplifier as the pulse energy can be much higher while the pulse peak power is clamped. Therefore, excessive nonlinear phase shift accumulation could be avoided as much as possible. Consequently, much larger pulse energy can be achieved based on DSR amplification. Combining with the master oscillator power amplifier (MOPA), Zheng et al reported a DSR pulse with 0.33 mJ pulse energy by using a figure-of-nine double-clad Tm-doped fiber laser in the 2 µm band [15].

One of the most representative properties of DSR pulses is the clamped pulse peak power and linear variation in pulse width with respect to the pump power change. The clamped pulse peak power makes DSR pulses immune from exhibition of period doubling, which is a threshold effect. As it is well-known, nonuniformity of a soliton pulse train caused by period bifurcation could be an intrinsic feature of all mode-locked fiber lasers [16]. Period bifurcation, which is also known

* lmzhao@ieee.org

as periodic pulsations, usually can be observed in the time domain where the output of the pulse train would show periodic changes in pulse parameters at the multiple cavity roundtrips. Experimental observation of period-doubling and -tripling bifurcation of mode-locked pulses in a fiber laser was firstly reported by Tamura et al. [17]. Since then, period bifurcation has experimentally been observed in fiber lasers with different scenarios of soliton pulses, such as dispersion-managed solitons [18], multiple solitons [19], bound solitons [20], gain-guided solitons [21] and vector solitons [22]. Theoretically, Akhmediev et al found the parameter regime of the CGLE where various periodic pulsating solitons could exist [23]. As a promising pulse energy boost mechanism, DSR pulses have been reported on multi-pulse states [24–26], harmonic mode-locking [27, 28] and the compressibility of DSR pulses [29]. We noticed that among all the above-mentioned researches DSR pulses temporally exhibit a uniform pulse train. Recently, Du et al numerically predicted the appearance of period doubling of DSR pulses in a fiber laser [30]. However, to the best of our knowledge, so far, no experimental demonstration of period doubling behaviors of DSR pulses has been reported.

In this paper, period doubling bifurcation of DSR pulses was first experimentally demonstrated with numerical reproduction. The DSR feature is lost during the transition from period one to period doubling. However, the DSR performance reappears once the period doubling was fully developed. That is, breach and recurrence of DSR operation exist during gain increasing. Experimental demonstration of period doubling bifurcation of DSR pulses was achieved in an Yb-doped all-normal-dispersion fiber laser. For the first time, we demonstrated the development of a uniform DSR pulse train transforming into a period-doubling bifurcation state with the increase in the pump power. Different from the conventional behaviour of the increase in the pulse peak difference between two adjacent pulses [17], DSR pulses in a period-doubling state maintain their pulse peak power while their pulse width linearly increases with respect to the pump power increase. To make the period-doubling of DSR pulses appearing, the pulse peak power of DSR pulses should be able to be increased in practice.

II. METHODS

The numerical simulation is carried out based on the fiber laser specially designed as shown in Fig. 1. The cavity is constructed by a 30/70 optical coupler (OC) connecting a unidirectional ring and a loop mirror. The transmission of the loop mirror will act as a sinusoidal function, initializing the mode-locking [9]. The 42-cm-long ytterbium-doped fiber (YDF) is pumped by a 600 mW, 976 nm laser diode (LD) through a wavelength division multiplexer (WDM). 20% of the intra-cavity power is output by a 20/80 OC. A polarization independent isolator is used to ensure the counter-clockwise propagation of light in the unidirectional ring. To carefully adjust the polarization state of the laser cavity, we employ the three-paddle PCs in both the unidirectional ring and the loop mirror. To enhance the nonlinearity, we insert a 200-m-long single mode fiber into the loop mirror. All fiber components in this fiber laser work in the normal dispersion regime.

The laser operation is simulated based on the roundtrip model [31]. The pulse propagation in fibers is governed by the CGLE:

$$\frac{\partial u}{\partial z} = -\frac{i\beta_2}{2}\frac{\partial^2 u}{\partial t^2} + i\gamma|u|^2 u + \frac{g}{2}u + \frac{g}{2\Omega_g^2}\frac{\partial^2 u}{\partial t^2} \qquad (1)$$

where u is the normalized electric field envelope; β_2 is the second-order dispersion coefficient, and gamma represents the nonlinearity of the fiber; t is the pulse local time and z is the propagation distance. g is the saturable gain of the fiber and Ω_g is the gain bandwidth. For the YDF, the gain saturation was considered as

$$g = \frac{G_0}{1+\int |u|^2 dt \Big/ E_{sat}} \qquad (2)$$

where G_0 is the small-signal-gain coefficient and E_{sat}=2 nJ is the saturation energy. The integration was carried out over the whole round-trip period.

The transmission of the NOLM was considered as [31]

$$T = \frac{1}{2}\left[1 - q\cos\left(\frac{\pi I(t)}{I_{sat}}\right)\right] \qquad (3)$$

where the modulation depth was set as q=0.4, $I(t)$ is the instantaneous pulse power, I_{sat} is the saturation power.

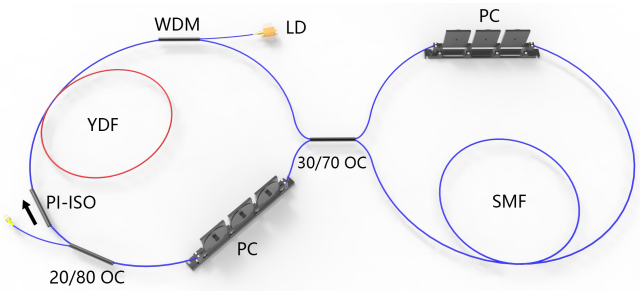

FIG. 1. Experimental setup of the fiber laser.

III. RESULTS AND DISCUSSIONS

A. Numerical Simulations

The DSR pulses can be easily achieved under the condition of small I_{sat} [31], for example, I_{sat}=200 W. As shown in Fig. 2, typical DSR feature, that the pulse peak power was clamped while the pulse duration broadened with gain increasing, was presented. Numerically

we already knew that the clamped pulse peak power can be higher if the saturation power was set larger [31]. However, when we set I_{sat}=250 W, period doubling was numerically obtained during we increased the small signal gain, as shown in Fig. 3(a). The pulse profile shuttled when the small signal gain coefficient was increased to G_0=40000. The pulses repeated themselves every two times of the cavity length, i.e., period doubling appears. We note that there is only one pulse existing in the cavity and the pulse duration was same for the adjacent roundtrip. Continuously increasing the small signal gain coefficient, within a range up to G_0=55000, typical DSR feature of linearly broadening of pulse duration was maintained while the period doubling bifurcation existed. Further increasing the small signal gain coefficient caused the dying of mode locking ultimately. Figure 3(b) shows the development of DSR pulses before period doubling (G_0<30000) and during period doubling (40000<G_0<50000).

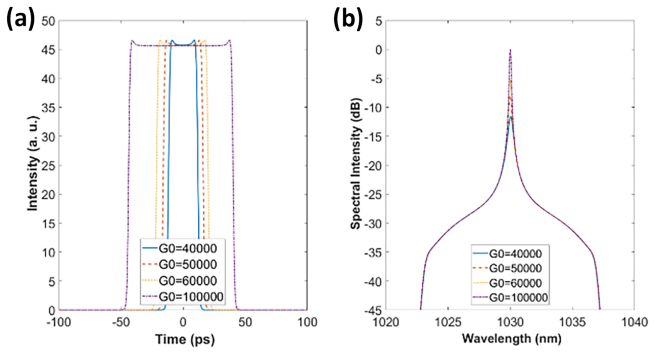

FIG. 2. (a) DSR pulse profiles and (b) spectra under different small signal gain when I_{sat}=200 W.

B. Experimental Results

Encouraged by the simulations, the laser of Fig. 1 was built. Firstly, we observed the generation of DSR pulses in the laser cavity. When the pump power reached the mode-locking threshold, mode-locked pulses at nanosecond-scale could rise from the continuous wave by appropriately setting the two PCs. Figure 4(a) shows the temporal trace of pulses monitored by using a high-speed photodetector (New focus 1014, 45-GHz) in combination with a digital oscilloscope (Agilent DSA-X 96204Q, 63-GHz). The response time of the monitor system is 20 ps. Started with pump power of 55.7 mW, the generated pulse showed a square-shaped temporal profile, with a pulse width of 631 ps. Further increasing the pump power, the trailing edge of the pulse broadened while the peak of pulse remained almost constant due to the peak power clamping (PPC) effect [32]. Figure 4(b) plots the change in temporal pulse width and average output power of the fiber laser when the pump power was increased from 55.7 to 129.5 mW. The pulse width

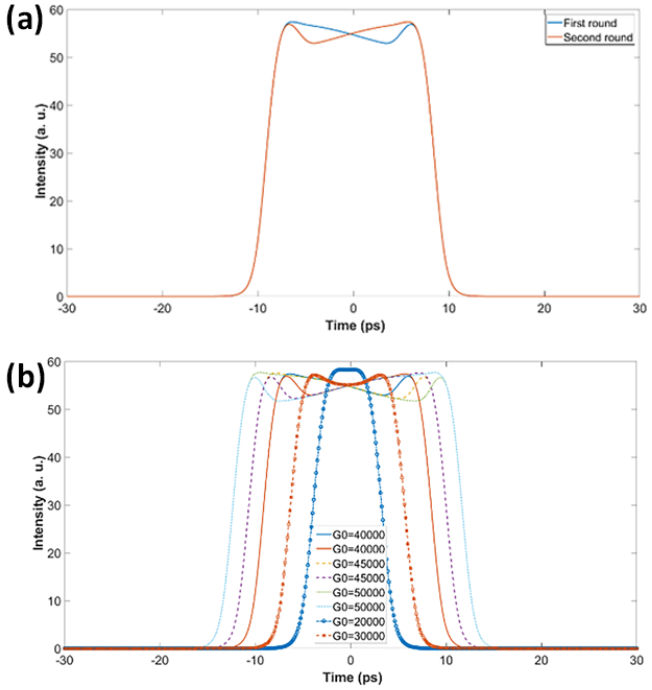

FIG. 3. DSR pulse profiles under period doubling bifurcation (a) when G_0=40000; (b) under various G_0, when I_{sat}=250 W.

increased linearly from 631 ps to 1.597 ns, and the average output power gradually increased from 0.18 to 0.496 mW. The linear change in these two parameters indicates that the calculated peak power of the pulse remained almost constant during the pulse broadening. The results showed the fingerprint of DSR pulses. Figure 4(c) shows the radio frequency (RF) spectrum detected by an analyzer (Agilent N9320B) with 1 MHz span and 10 Hz resolution bandwidth (RBW) when the pump power was increased to 129.5 mW. The first order of the RF spectrum peaked at 900 kHz, which corresponded to the cavity fundamental repetition frequency. The signal-to-noise ratio increased from 60.6 dB when the pump power was 55.7 mW to 69.5 dB when the pump power was 129.5 mW. With the 10 MHz span and 1 kHz RBW, the trace of RF spectrum showed a uniform degradation as plotted in Fig. 4(d). The RF spectrum confirms that the single DSR pulse operated in a stable state.

Figure 5(a) shows the oscilloscope trace of temporal pulse train with the pump power of 129.5 mW. A uniform pulse train can be observed as pulses with equal intensity repeatedly showed up every cavity roundtrip. The period is 1.11 µs, in agreement with the reciprocal of the cavity fundamental repetition rate. With fixed settings of PCs, the uniform state of the pulse train could be maintained when we increased the pump power only. However, when the pump power was increased to 260.6 mW, the intensity of the pulse started to have a periodic difference. As shown in Fig. 5(b), although the pulse was still mode-locked at the cavity period, the pulse

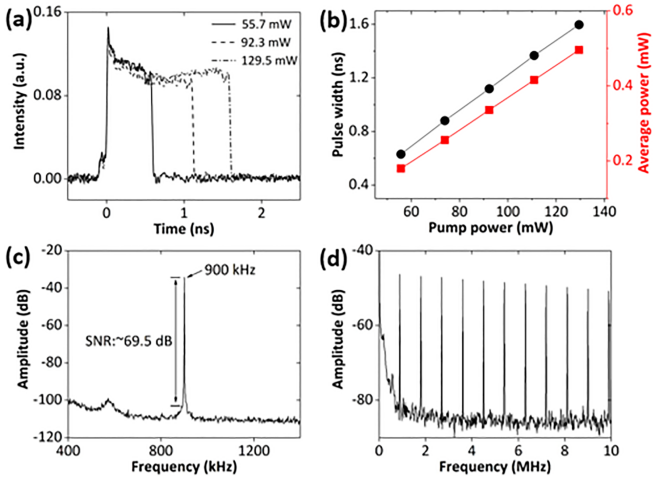

FIG. 4. (a) DSR pulse profiles and (b) pulse width and average output power change versus pump power; (c) RF spectrum with span of 1 MHz; (d) RF spectrum with span of 10 MHz.

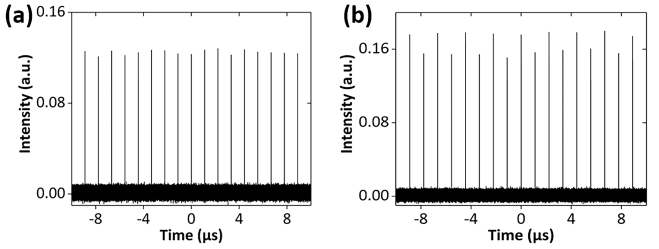

FIG. 5. The oscilloscope trace of the DSR pulse train at (a) period-one state; (b) period-two state.

intensity varies vividly every two cavity roundtrips. It suggested that the DSR pulse exhibited the property of period-doubling bifurcation in the time domain.

When the period-doubling bifurcation occurs, new frequency component simultaneously appears on the RF spectrum [24]. To confirm the generation of period-doubling bifurcation, we measured the RF spectrum of the pulse train with the pump power of 260.6 mW. Figure 6(a) plots the RF spectrum with 10 MHz span and 1kHz RBW. Compared with Fig. 4(d), there were newly generated frequency components locating at the half of the

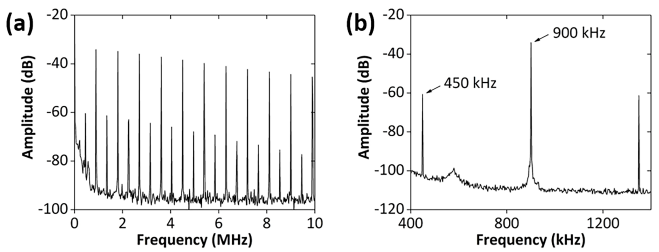

FIG. 6. The RF spectrum of period-two state with (a) 10 MHz span; (b) 1 MHz span.

cavity fundamental repetition frequency and its higher order harmonics. Figure 6(b) plots the detailed RF spectrum with 1 MHz span and 10 Hz RBW. The first order of the RF spectrum jumped from 900 kHz to 450 kHz. The pulse train we obtained at the pump power of 260.6 mW was operating in a so-called period-two state.

C. Discussions

It is well-known that the appearance of period-doubling is one of the intrinsic nonlinear properties of fiber lasers and it is a threshold effect [33]. The nonlinearity in a fiber laser could be identified by the accumulated nonlinear phase shift during the pulse propagation in a fiber laser, which is proportional to the nonlinear coefficient, the pulse peak power, and the propagation length [34]. For a fiber laser, the pulse peak power generally increases with respect to the increase in the pump power, therefore enhancing the accumulated nonlinear phase shift. Consequently, the appearance of period-doubling is possible. For a fiber laser generating DSR pulses, as the pulse peak will be kept constant during the pump power increase, it is out of our expectation for the appearance of period-doubling.

To get insight of the generation of period-doubling of DSR pulses, detailed experimental analyses were carried out. We were back to Fig. 4 and found that there indeed exists a slight pulse peak power increasing with the pump power. The pulse peak power increased from 0.317 W to 0.345 W when the pump power increased from 55.7 mW to 129.5 mW. Therefore, even under the DSR operation, it is still possible to increase pulse peak power while the pulse peak power is supposed to be clamped. However, this kind of pulse peak power improvement is slight and limited. It is almost impossible to achieve the stepping over the threshold requirement for the generation of period-doubling. Recently we found that in a DSR pulse fiber laser, it is possible to achieve DSR pulse breaking, DSR pulse harmonic mode locking, or DSR pulse narrowing by solely increasing the pump power [35]. It is resulted from the multiple parameter changes caused by solely increasing the pump power. Theoretically, the solely increase in the gain will result in the fingerprint behavior of DSR pulses – linearly broadening of pulse width with clamped pulse peak power [1, 5, 31]. However, in practice, the sole increase in the pump power may cause multiple parameter changes apart from the expected gain increase only [35], leading to the change in pulse profile. Experimentally we measured the pulse profile when we increased the pump power from 129.5 mW to 242 mW. As shown in Fig. 7, it is found that both the width and the peak of the pulse increased while the pulse train is still under period-one state. Further increasing the pump power, as long as the pulse peak power can be improved to fulfill the nonlinearity threshold requirement, period-doubling of DSR pulses can be achieved in the fiber laser as shown in Fig. 3(b).

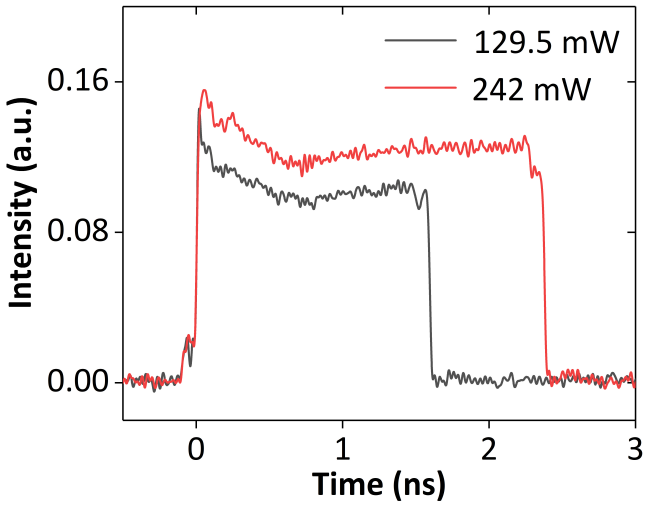

FIG. 7. Pulse profiles of the DSR pulse at pump power of 129.5 mW and 242 mW, respectively.

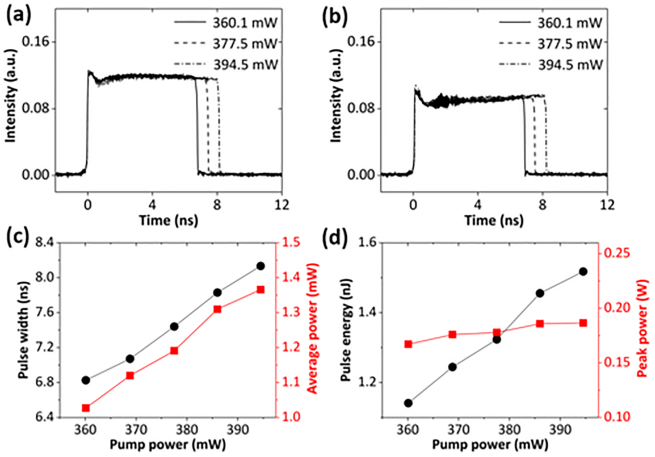

FIG. 8. DSR pulse broadening in the period-doubling state with increasing pump power. (a) High-intensity pulse profile; (b) Low-intensity pulse profile; (c) Pulse width and average output power versus pump power; (d) Pulse energy and pulse peak power versus pump power.

It is interesting to know the dynamics of DSR pulses operated in period-doubling state. After the pulse train was transformed into the period-doubling state, we recorded the detailed temporal traces of the adjacent high- and low-intensity pulses. We found that the PPC effect continue to play a role after the period-doubling operation was achieved. In another word, the DSR performance could be maintained even after the period-doubling operation is achieved. With another fixed settings of PCs, we found a pump power regime where the pulses exhibiting the period-doubling state showed typical characteristics of DSR pulse broadening. As shown in Fig. 8(a) and Fig. 8(b), the pulse profiles of the high-/low- intensity pulse suggest that DSR pulses experiencing period-doubling had same pulse width at fixed-level of pump power, which matched well with numerical simulations of Fig. 3. The pulse width was temporally broadened from 6.83 to 8.13 ns when the pump power was increased from 360.1 to 394.5 mW. Linear pulse parameter changes and PPC effect can be retrieved from Fig. 8(c) and Fig. 8(d), which clearly demonstrates the DSR performance. We note that the DSR broadening process under the period-doubling state only exists within a very narrow pump power tuning range of 35 mW here. Larger pump power will make the DSR pulse unstable until dying out. Numerical results were reproduced again.

Experimentally we also observed the phenomenon of DSR pulse narrowing under period-doubling state. As shown in Fig. 9, the pulse width of both the high-intensity pulses and the low-intensity one reduced when the pump power was increased from 260.6 to 297.4 mW. The pulse widths of both pulses started to shrink while the peak of the pulse remained constant as the pump power increased. The pulse narrowing phenomenon of a DSR pulse has been reported previously, which is caused by the gain competition in the laser [34]. We note that the high and low intensity pulse always had the same pulse width during the pulse narrowing. The evolution suggests that the pulses exhibiting period-doubling behavior can show the characteristics of DSR pulses no matter it is a DSR broadening or narrowing. The pulse would become unstable when the pump power was beyond 315.6 mW.

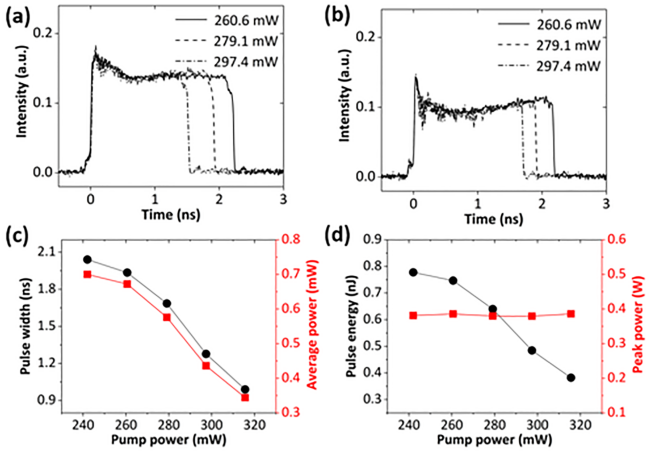

FIG. 9. DSR pulse narrowing in the period-doubling state with increasing pump power (see also Visualization 2). (a) High-intensity pulse profile; (b) Low-intensity pulse profile; (c) Pulse width and average output power versus pump power; (d) Pulse energy and pulse peak power versus pump power.

IV. CONCLUSIONS

In conclusion, we have, for the first time, experimentally observed period doubling of DSR pulses in a fiber laser. The contradiction between the clamped pulse peak

power of DSR performance and the required increasing nonlinearity for the appearance of period doubling was overcome by the simultaneous change of multiple parameters resulted from the increasing pump power. Therefore, DSR pulses can transform into the period-doubling state by simply increasing the pump power. Temporally, DSR pulses in the period-doubling state had two sets of the pulse parameters in the adjacent cavity roundtrip. Both numerical results and experimental observations confirm that in a fiber laser, the pulse can simultaneously exhibit the phenomena of DSR and period-doubling bifurcation. It was shown that DSR pulses exhibiting period-doubling could maintain their peak during the process of pulse broadening or pulse narrowing with respect to the pump power increase. The findings enrich the dynamics of DSR pulses, which will benefit the design of ultrafast lasers with desirable soliton patterns for practical applications.

ACKNOWLEDGMENTS

This research is supported by National Natural Science Foundation of China (NSFC) (11674133, 11911530083, 61575089); Fundamental Research Funds for the Central Universities (HUST: 2020kfyXJJS007); Russian Foundation for Basic Research (RFBR) (19-52-53002); Royal Society (IE161214); Protocol of the 37th Session of China-Poland Scientific and Technological Cooperation Committee (37-17); European Union's Horizon 2020 research and innovation programme under the Marie Skłodowska-Curie grant agreement No. 790666. Mariusz Klimczak acknowledges support from Fundacja na rzecz Nauki Polskiej (FNP) in scope of First TEAM/2016-1/1 (POIR.04.04.00-00-1D64/16).

[1] W. Chang, A. Ankiewicz, J. M. Soto-Crespo, and N. Akhmediev, Dissipative soliton resonances, Phys. Rev. A **78**, 023830 (2008).
[2] Y. Song, S. Chen, Q. Zhang, L. Li, L. Zhao, H. Zhang, and D. Tang, Vector soliton fiber laser passively mode locked by few layer black phosphorus-based optical saturable absorber, Optics express **24**, 25933 (2016).
[3] B. Guo, S.-H. Wang, Z.-X. Wu, Z.-X. Wang, D.-H. Wang, H. Huang, F. Zhang, Y.-Q. Ge, and H. Zhang, Sub-200 fs soliton mode-locked fiber laser based on bismuthene saturable absorber, Optics express **26**, 22750 (2018).
[4] Y. Song, X. Shi, C. Wu, D. Tang, and H. Zhang, Recent progress of study on optical solitons in fiber lasers, Applied Physics Reviews **6**, 021313 (2019).
[5] X. Wu, D. Tang, H. Zhang, and L. Zhao, Dissipative soliton resonance in an all-normal-dispersion erbium-doped fiber laser, Optics express **17**, 5580 (2009).
[6] S.-K. Wang, Q.-Y. Ning, A.-P. Luo, Z.-B. Lin, Z.-C. Luo, and W.-C. Xu, Dissipative soliton resonance in a passively mode-locked figure-eight fiber laser, Optics express **21**, 2402 (2013).
[7] K. Krzempek, J. Sotor, and K. Abramski, Compact all-fiber figure-9 dissipative soliton resonance mode-locked double-clad er: Yb laser, Optics letters **41**, 4995 (2016).
[8] Y. Guo, Y. Xu, J. Zhang, and Z. Zhang, High-power dissipative soliton resonance fiber laser with compact linear-cavity configuration, Optik **181**, 13 (2019).
[9] N. Doran and D. Wood, Nonlinear-optical loop mirror, Optics letters **13**, 56 (1988).
[10] K. Krzempek, D. Tomaszewska, and K. M. Abramski, Dissipative soliton resonance mode-locked all-polarization-maintaining double clad er: Yb fiber laser, Optics express **25**, 24853 (2017).
[11] Z. Cheng, H. Li, H. Shi, J. Ren, Q.-H. Yang, and P. Wang, Dissipative soliton resonance and reverse saturable absorption in graphene oxide mode-locked all-normal-dispersion yb-doped fiber laser, Optics Express **23**, 7000 (2015).
[12] H. Yang and X. Liu, Ws2-clad microfiber saturable absorber for high-energy rectangular pulse fiber laser, IEEE Journal of Selected Topics in Quantum Electronics **24**, 1 (2017).
[13] H. Lee, Monolayer mos2-based high energy rectangular pulse fiber laser, Optik **174**, 530 (2018).
[14] G. Semaan, F. B. Braham, J. Fourmont, M. Salhi, F. Bahloul, and F. Sanchez, 10 μj dissipative soliton resonance square pulse in a dual amplifier figure-of-eight double-clad er: Yb mode-locked fiber laser, Optics letters **41**, 4767 (2016).
[15] Z. Zheng, D. Ouyang, X. Ren, J. Wang, J. Pei, and S. Ruan, 0.33 mj, 104.3 w dissipative soliton resonance based on a figure-of-9 double-clad tm-doped oscillator and an all-fiber mopa system, Photonics Research **7**, 513 (2019).
[16] B. Zhao, D. Y. Tang, L. M. Zhao, P. Shum, and H. Y. Tam, Pulse-train nonuniformity in a fiber soliton ring laser mode-locked by using the nonlinear polarization rotation technique, Phys. Rev. A **69**, 043808 (2004).
[17] K. Tamura, C. Doerr, H. Haus, and E. Ippen, Soliton fiber ring laser stabilization and tuning with a broad intracavity filter, IEEE photonics technology letters **6**, 697 (1994).
[18] L. Zhao, D. Tang, F. Lin, and B. Zhao, Observation of period-doubling bifurcations in a femtosecond fiber soliton laser with dispersion management cavity, Optics express **12**, 4573 (2004).
[19] L. Zhao, D. Tang, T. Cheng, and C. Lu, Period-doubling of multiple solitons in a passively mode-locked fiber laser, Optics communications **273**, 554 (2007).
[20] L. Zhao, D. Tang, and B. Zhao, Period-doubling and quadrupling of bound solitons in a passively mode-locked fiber laser, Optics communications **252**, 167 (2005).
[21] L. Zhao, D. Tang, X. Wu, and H. Zhang, Period-doubling of gain-guided solitons in fiber lasers of large net normal dispersion, Optics communications **281**, 3557 (2008).
[22] L. Zhao, D. Tang, H. Zhang, X. Wu, C. Lu, and H. Tam, Period-doubling of vector solitons in a ring fiber laser, Optics communications **281**, 5614 (2008).
[23] N. Akhmediev, J. M. Soto-Crespo, and G. Town, Pulsating solitons, chaotic solitons, period doubling, and pulse

coexistence in mode-locked lasers: Complex ginzburg-landau equation approach, Physical Review E **63**, 056602 (2001).

[24] A. Komarov, F. Amrani, A. Dmitriev, K. Komarov, and F. Sanchez, Competition and coexistence of ultrashort pulses in passive mode-locked lasers under dissipative-soliton-resonance conditions, Physical Review A **87**, 023838 (2013).

[25] Y. Lyu, X. Zou, H. Shi, C. Liu, C. Wei, J. Li, H. Li, and Y. Liu, Multipulse dynamics under dissipative soliton resonance conditions, Optics express **25**, 13286 (2017).

[26] S. D. Chowdhury, A. Pal, S. Chatterjee, R. Sen, and M. Pal, Multipulse dynamics of dissipative soliton resonance in an all-normal dispersion mode-locked fiber laser, Journal of Lightwave Technology **36**, 5773 (2018).

[27] Y. Lyu, H. Shi, C. Wei, H. Li, J. Li, and Y. Liu, Harmonic dissipative soliton resonance pulses in a fiber ring laser at different values of anomalous dispersion, Photonics Research **5**, 612 (2017).

[28] C. Shang, X. Li, Z. Yang, S. Zhang, M. Han, and J. Liu, Harmonic dissipative soliton resonance in an yb-doped fiber laser, Journal of Lightwave Technology **36**, 4932 (2018).

[29] D. Li, L. Li, J. Zhou, L. Zhao, D. Tang, and D. Shen, Characterization and compression of dissipative-soliton-resonance pulses in fiber lasers, Scientific reports **6**, 23631 (2016).

[30] W. Du, H. Li, Y. Lyu, C. Wei, and Y. Liu, Period doubling of dissipative-soliton-resonance pulses in passively mode-locked fiber lasers, Frontiers in Physics **7**, 253 (2019).

[31] D. Li, D. Tang, L. Zhao, and D. Shen, Mechanism of dissipative-soliton-resonance generation in passively mode-locked all-normal-dispersion fiber lasers, Journal of Lightwave Technology **33**, 3781 (2015).

[32] D. Y. Tang, L. M. Zhao, B. Zhao, and A. Q. Liu, Mechanism of multisoliton formation and soliton energy quantization in passively mode-locked fiber lasers, Phys. Rev. A **72**, 043816 (2005).

[33] L. Zhao, C. Shu, Y. Wang, and L. Li, Research progress of period doubling bifurcation in ultrafast fiber lasers (invited), Infrared and Laser Engineering **47**, 803002 (2018).

[34] G. P. Agrawal, *Nonlinear fiber optics* (Elsevier, 2013).

[35] Y. Wang, L. Li, J. Zhao, S. Wang, C. Shu, L. Su, D. Tang, D. Shen, and L. Zhao, Unusual evolutions of dissipative-soliton-resonance pulses in an all-normal dispersion fiber laser, IEEE Photonics Journal **11**, 1 (2019).